



# Imaging and tissue biodistribution of $^{99m}\text{Tc}$ -labeled adenovirus knob (serotype 5)

KR Zinn<sup>1</sup>, JT Douglas<sup>2</sup>, CA Smyth<sup>1</sup>, H-G Liu<sup>1</sup>, Q Wu<sup>1</sup>, VN Krasnykh<sup>2</sup>, JD Mountz<sup>3</sup>, DT Curiel<sup>2</sup> and JM Mountz<sup>1</sup>

<sup>1</sup>Division of Nuclear Medicine, Department of Radiology, <sup>2</sup>Gene Therapy Program, and <sup>3</sup>Division of Rheumatology, Department of Internal Medicine, University of Alabama at Birmingham Medical Center, Birmingham, AL, USA

Hepatic sequestration of systemically administered adenoviral vectors reduces the number of viral particles available for delivery to other tissues. The biological basis of this phenomenon was investigated using a new *in vivo* technique which permitted imaging in real time. Recombinant adenovirus serotype 5 knob (Ad5K) was radiolabeled with the gamma-emitter  $^{99m}\text{Tc}$  (half-life = 6 h). Scatchard analysis of the  $^{99m}\text{Tc}$ -Ad5K showed specific, high-affinity binding to U293 cells ( $K_d = 1.4 \pm 0.5 \text{ nM}$ ), demonstrating that the radiolabeling process had no effect on receptor binding. *In vivo* dynamic imaging with an Anger gamma camera revealed that the liver binding followed an exponential rise to maximum, with a measured 100% extraction efficiency. Initially, the liver binding capacity

was  $3.1 \pm 0.4 \mu\text{g Ad5K}$ , equivalent to approximately 17 000 Ad5K molecules per liver cell. Liver binding was blocked by preincubation of Ad5K with neutralizing anti-Ad5K antibody; a 50% reduction in liver uptake was demonstrated by imaging. Unlabeled Ad5K was more effective in blocking liver uptake of  $^{99m}\text{Tc}$ -Ad5K, whereas irrelevant unlabeled Ad3K had no effect. Imaging data for the liver uptake studies were in agreement with biodistribution determined by removing and measuring tissues. These data demonstrated that *in vivo* imaging is a sensitive tool for measuring changes to liver tropism. Similar imaging techniques can be applied to adenovirus vectors to measure specific targeting for gene therapy.

**Keywords:** adenovirus knob; imaging;  $^{99m}\text{Tc}$

## Introduction

The ability of recombinant adenoviral vectors of serotypes 2 (Ad2) and 5 (Ad5) to accomplish efficient gene transfer to a range of cell types *in vivo* is being exploited in the development of gene therapy approaches. These approaches are for the treatment of inherited and acquired genetic diseases, as well as to treat carcinomas of various organs. Among viral vectors, adenoviruses possess the unique attribute of stability in the bloodstream, a feature which should permit development of the adenovirus as a gene therapy vector which can be administered to the patient simply by intravenous injection.<sup>1,2</sup> However, intravenous administration of the present generation of Ad vectors delivers more than 90% of the input virus to the liver, thereby reducing the titer of virus particles available for transduction of the target disease cells.<sup>2–4</sup> Therefore, it will be necessary to overcome this problem of hepatic sequestration if the adenovirus is to realize its potential as an effective vector for gene therapy. It will then be possible to approach a second limitation of the adenovirus, the fact that the widespread distribution of the primary cellular receptor precludes the targeting of specific cell types. This allows ectopic expression of the delivered therapeutic gene, with

possibly deleterious consequences. Therefore, a number of investigators are attempting to alter the tropism of the Ad vector to permit gene delivery to certain target cell types.<sup>5–10</sup>

An understanding of the biological basis of the sequestration of Ad by the liver should yield strategies to avoid this occurrence. While this mechanism has not been investigated, a number of studies have elucidated the pathway of Ad cellular infection. The initial high-affinity binding of Ad2 and Ad5 to the primary cellular receptor occurs via the knob domain of the trimeric fiber capsid protein, as demonstrated by the ability of recombinant knob or anti-knob antibodies to inhibit Ad infection.<sup>11–13</sup> Two receptors for Ad5 have been identified.<sup>14,15</sup> Following attachment, the next step in infection by Ad2 and Ad5 is internalization of the virion by receptor-mediated endocytosis, a process involving the lower affinity of Arg-Gly-Asp (RGD) peptide sequences in the penton base to secondary host cell receptors, integrins  $\alpha_v\beta_3$  and  $\alpha_v\beta_5$ .<sup>16,17</sup> Thus, the major determinant of Ad tropism is the initial high-affinity interaction between the knob domain of the fiber protein and its cognate cellular receptor.

In this study, we examined the biodistribution of the Ad5 knob (Ad5K) in mice following intravenous injection. This was achieved by radiolabeling recombinant trimeric Ad5K with technetium-99m ( $^{99m}\text{Tc}$ ), imaging the *in vivo* biodistribution with an Anger gamma camera, and measuring the tissue levels of radioactivity following termination of the animals. We show that the uptake of

$^{99m}\text{Tc}$ -Ad5K by the liver was significantly reduced upon coinjection of neutralizing anti-Ad5K monoclonal antibody or unlabeled Ad5K, but was not affected by the knob of Ad serotype 3 (Ad3K), which recognizes a different primary receptor.<sup>18,19</sup>

## Results

### SDS-PAGE

The results for SDS-PAGE analysis of the  $^{99m}\text{Tc}$ -labeled Ad5K are displayed in Figure 1. Two identical gels were run. One gel was stained for protein with Coomassie Brilliant Blue. The other gel was dried and radioactivity was detected by autoradiography using phosphor imaging. The molecular mass of the single band for Ad5K detected by autoradiography could be determined since an adjacent lane contained proteins of known molecular mass (data not shown). Both protein staining and autoradiography demonstrated that a single, major band for Ad5K was located at a molecular mass (63 kDa) consistent with the trimeric knob. Quantitative analysis of the phosphor counts obtained by autoradiography showed that 94% of the applied activity was present as the trimeric form.

### Scatchard analysis

Scatchard analysis of the  $^{99m}\text{Tc}$ -Ad5K showed specific binding to U293 cells; the  $K_d$  averaged  $1.4 \pm 0.5$  nM ( $n =$

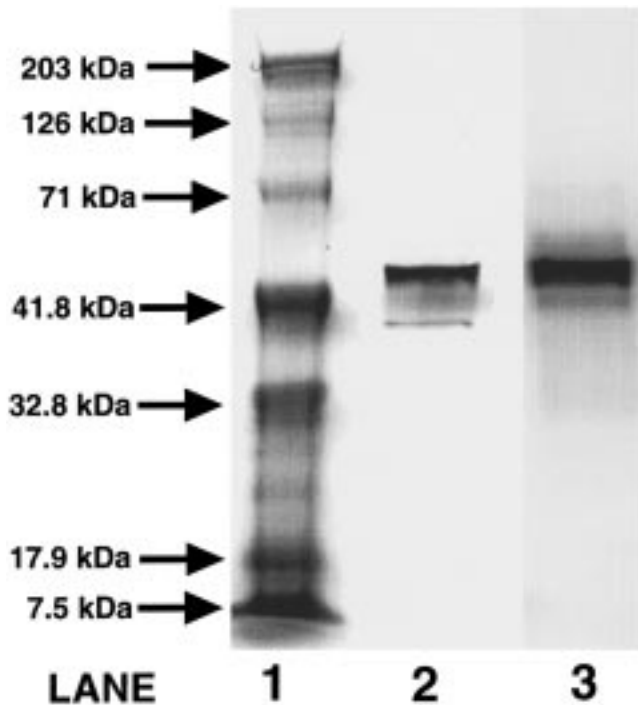


**Figure 1** SDS-PAGE of  $^{99m}\text{Tc}$ -labeled Ad5K. Proteins in lane 1 (molecular weight markers) and lane 2 (Ad5K after  $^{99m}\text{Tc}$  labeling) were stained with Coomassie Brilliant Blue and the gel was scanned. A second identical gel was dried and radioactivity was detected by autoradiography using phosphor imaging. The  $^{99m}\text{Tc}$  activity bound to Ad5K is shown in lane 3. Quantitative analysis of lane 3 phosphor counts showed that 94% of the activity was bound to the trimeric Ad5K.

3). Figure 2 shows two representative Scatchard plots; the inverse of the slope of each line is equal to the dissociation constant ( $K_d$ ) for the knob and its receptor. Binding of the  $^{99m}\text{Tc}$ -Ad5K was specific, since it was completely inhibited by addition of 100-fold excess Ad5K. The binding of Ad5K to its cellular receptor was not changed by the radiolabeling process.

### Dynamic imaging of $^{99m}\text{Tc}$ -Ad5K

Dynamic imaging studies were conducted during the first 5 min after injection of  $12 \mu\text{g}$  of  $^{99m}\text{Tc}$ -Ad5K in four anesthetized mice. Figure 3 shows an example of the sequential images collected (5 s per frame) following injection of the  $^{99m}\text{Tc}$ -Ad5K into the tail vein (data were collected from mouse 1). The sequential images clearly show the  $^{99m}\text{Tc}$ -Ad5K first in the caudal vena cava, then the heart, with rapid subsequent binding by the liver.

Liver uptakes of  $^{99m}\text{Tc}$ -Ad5K in the four mice are presented in Figure 4. These liver uptake data were corrected for  $^{99m}\text{Tc}$ -Ad5K in the blood within, but not bound to, the liver. The technique for making this correction is discussed in Materials and methods. The liver uptake data were fit to the exponential rise to maximum equation ( $y = a(1 - e^{-bx}) + c$ ), with  $1/b$  equal to the time constant to reach maximum. The average time constant for mice 2–4 was  $22.7 \pm 3.3$  s. Mouse 1 was not included in this average due to a slower intravenous (i.v.) injection than the other three mice. Overall, the liver binding averaged  $29 \pm 2\%$  of the injected dose ( $n = 4$ ), with an initial (1 min) total binding capacity of  $3.1 \pm 0.4 \mu\text{g}$ .

### Dose-dependent liver accumulation of $^{99m}\text{Tc}$ -Ad5K

Mice were i.v. injected with either  $0.57 \mu\text{g}$  or  $12 \mu\text{g}$  of  $^{99m}\text{Tc}$ -Ad5K and killed 10 min later. Mice injected with the lower dose of  $^{99m}\text{Tc}$ -Ad5K were imaged between 3 and 10 min after dosing. The percentage of activity in the liver region of interest for these mice averaged  $81 \pm 3\%$  ( $n = 3$ ).

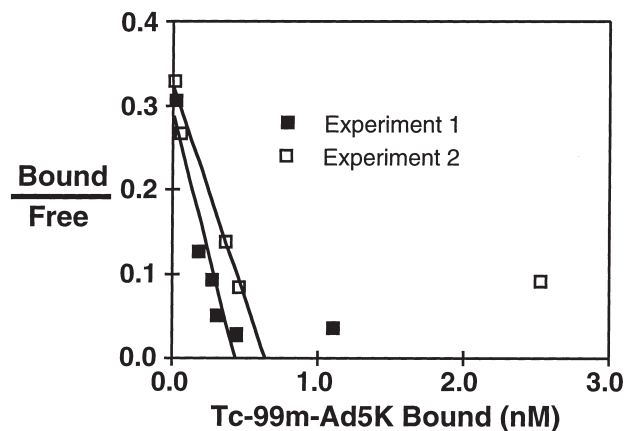


**Figure 2** Scatchard analysis of  $^{99m}\text{Tc}$ -Ad5K binding to U293 cells. Cells ( $0.4\text{--}1 \times 10^6$  per tube) were incubated for 2 h at  $4^\circ\text{C}$  with five to six different concentrations of  $^{99m}\text{Tc}$ -Ad5K, in the absence or presence of 100-fold excess unlabeled Ad5K. Cell-bound  $^{99m}\text{Tc}$ -Ad5K was determined after washing two times with PBS. Nonspecific binding accounted for less than 5% of binding. The specific activity for the  $^{99m}\text{Tc}$ -Ad5K ranged from 0.7 to  $3.3 \text{ MBq}/\mu\text{g}$  protein, with protein bound  $^{99m}\text{Tc}$  greater than 99% as determined by TLC analysis. The  $^{99m}\text{Tc}$ -labeled Ad5K inhibited infection of U293 cells with Ad5 at comparable concentrations to the unlabeled Ad5K.

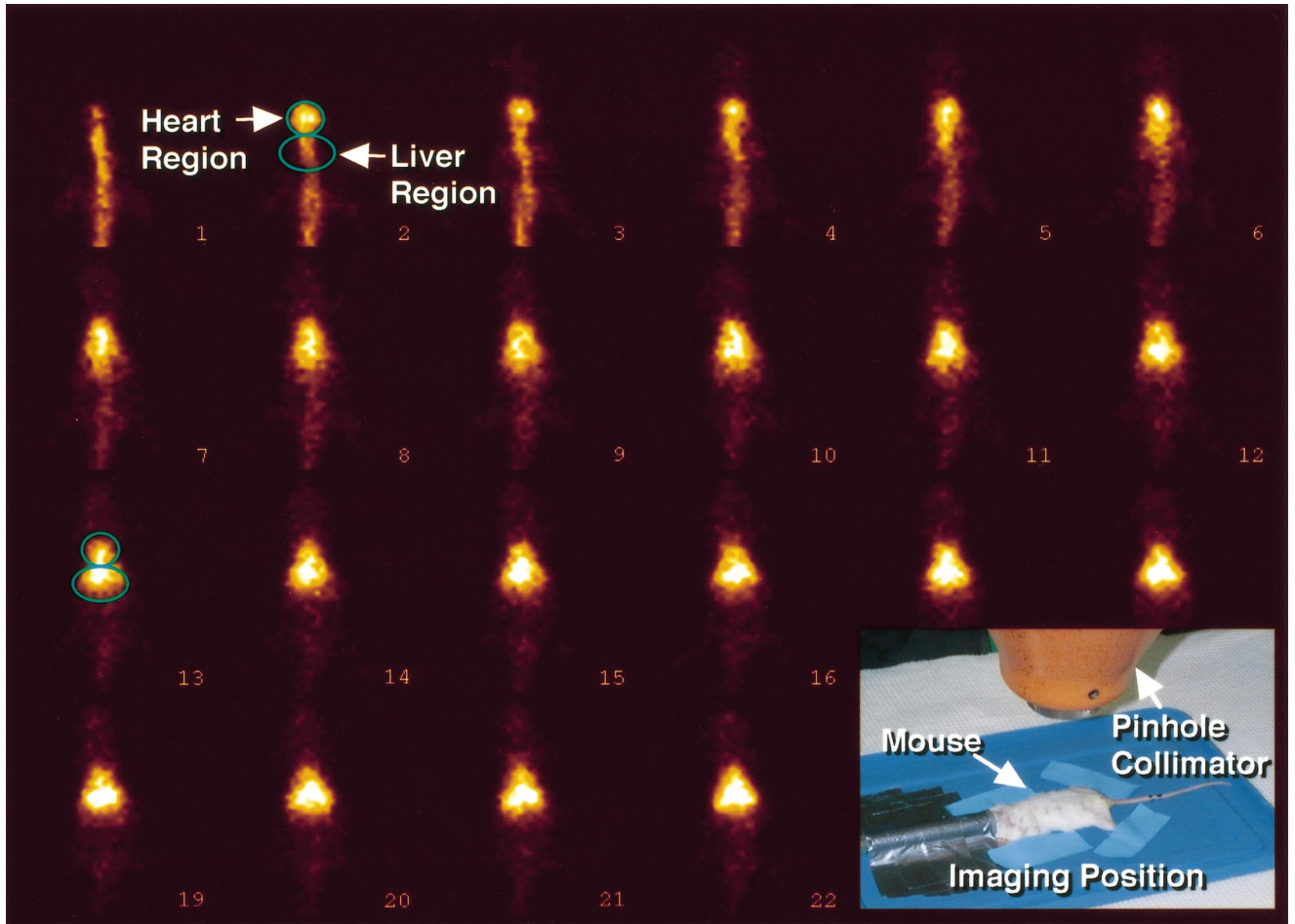


**Figure 3** Dynamic imaging of <sup>99m</sup>Tc-Ad5K in a mouse. This figure shows an example of sequential images collected every 5 s in a mouse i.v. injected (tail vein) with <sup>99m</sup>Tc-Ad5K. Regions drawn in frame 2 show radioactivity mainly in the heart, with activity in the liver region due to venous return via the caudal vena cava. Frame 13 shows activity in both the heart and liver regions of interest. The insert in the lower right corner shows the position of the anesthetized mouse during the dynamic imaging procedure.

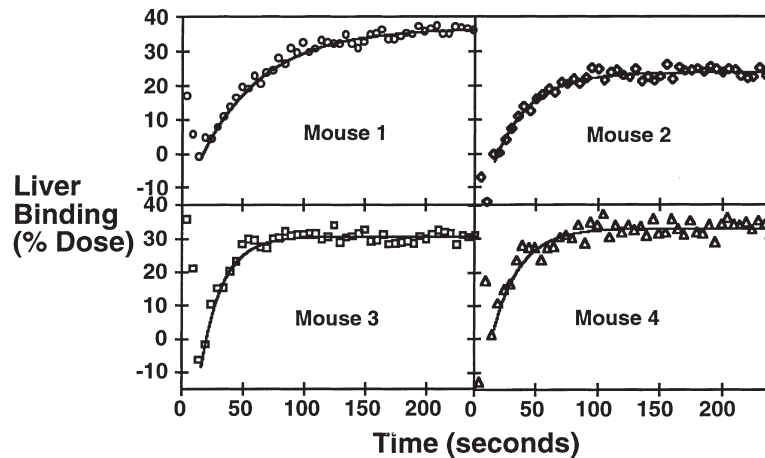


**Figure 4** Dynamic imaging of liver uptake for <sup>99m</sup>Tc-Ad5K in four mice. The liver uptake of <sup>99m</sup>Tc-Ad5K was calculated from the sequential dynamic images. The heart region, a measure of <sup>99m</sup>Tc-Ad5K in the blood, was used to correct the counts in the liver region that were due to blood. The technique is described in Materials and methods. Curves represent the best fit of the exponential rise to maximum equation ( $y = a(1 - e^{-bx}) + c$ ).

Table 1 summarizes tissue data from the mice killed 10 min following injection of <sup>99m</sup>Tc-Ad5K. At that time, 81 ± 3.5% of the lower dose of <sup>99m</sup>Tc-knob was present in the liver, the same finding as seen in the region of interest analysis from imaging. For the higher dose of <sup>99m</sup>Tc-Ad5K, 53 ± 1% was found in the liver, a value significantly higher than that determined from imaging (29%) at 2 min after dosing. The 53% value was likely higher because it included the liver-bound <sup>99m</sup>Tc-Ad5K as well as <sup>99m</sup>Tc-Ad5K in the blood.

Mice were injected with <sup>99m</sup>Tc-human serum albumin (HSA, 6.5 μg protein), a nuclear medicine blood pool agent (Table 1). At 10 min, 96.5 ± 8% of the dose was present in the blood compartment using 7% of body weight as the blood volume. The <sup>99m</sup>Tc-labeled HSA in the liver (from blood) accounted for 13.4% of the dose. Additional mice (n = 3) were injected with a 13-fold lower dose of <sup>99m</sup>Tc-labeled HSA (0.5 μg) to determine if the percentage of dose found in liver was affected by dose. Following termination, the liver accounted for 13.5 ± 1.6% of the lower dose, a value not significantly different than that found for the higher dose of <sup>99m</sup>Tc-labeled HSA. This finding allays any concern that organ distribution from blood-pool tracers are altered by dose levels.

For an additional comparison, mice (n = 3) were injected with <sup>99m</sup>Tc sulfur colloid (Technecoll; Mallinckrodt, St Louis, MO, USA), a nuclear medicine radiotracer commonly employed to image the reticulo-endothelial system (RES). These mice were also killed after 10 min, and data are presented in Table 1. The liver and spleen showed binding of 82.2 and 4.2% of the dose, respectively.

Three additional groups of mice were injected with a

higher dose of <sup>99m</sup>Tc-Ad5K (12 μg): with radiotracer alone, with co-injection of 1.0 mg Ad5K, or with co-injection of 0.8 mg Ad3K. The mice were imaged three times before termination at 1 h after injection. Results from imaging are presented in Figure 5, and indicate that only the addition of unlabeled Ad5K decreased the liver accumulation of <sup>99m</sup>Tc-Ad5K. Data are presented in Table 2 for these three groups after termination. Figure 6 summarizes the results for the liver, and includes the data for the 10 min termination as well. The percentage of dose in the liver for the <sup>99m</sup>Tc-Ad5K alone significantly increased to 64.5 ± 3.0% at 1 h, as compared with values at 10 min. Co-injection of Ad5K with the <sup>99m</sup>Tc-Ad5K significantly reduced the liver accumulation at 1 h from 64.5% to 24.3 ± 4.2% of the dose. The difference between 64.5 and 24.3% would appear to be an approximately 60% reduction. The true reduction is actually larger than 60% for the following reasons. A complete block of the liver binding of the <sup>99m</sup>Tc-labeled knob would still result in about 13.4% of the dose being present in the liver, due to blood in the liver. For that reason the <sup>99m</sup>Tc-HSA was included in Figure 5. The Ad5 knob inhibitor increased the amount of <sup>99m</sup>Tc-Ad5K in the blood to 54% of the dose. That amount in the blood would result in 7.2% of the dose in the liver due to blood in the liver (13.4% × 0.54). Therefore the Ad5K inhibitor decreased the liver binding from 64.5% to 17.1% (24.3–7.2%). This value is approximately a 75% reduction. The addition of Ad3K to the dose had no effect on liver accumulation of <sup>99m</sup>Tc-Ad5K.

The data for liver to blood (L:B) ratios are presented in Figure 7. <sup>99m</sup>Tc-Ad5K administered alone had a blood ratio of 5.8 at 1 h, which is significantly increased from

**Table 1** Biodistribution of <sup>99m</sup>Tc-Ad5K, <sup>99m</sup>Tc-HSA and <sup>99m</sup>Tc-sulfur colloid 10 min after dosing

Organ or tissue	Mice dosed with <sup>99m</sup> Tc-Ad5K (0.57 μg)		Mice dosed with <sup>99m</sup> Tc-Ad5K (12 μg)		Mice dosed with <sup>99m</sup> Tc-HSA		Mice dosed with <sup>99m</sup> Tc-sulfur colloid	
	Bq/g mean (s.e.m.) × 1000	% of dose mean (s.e.m.)	Bq/g mean (s.e.m.) × 10000	% of dose mean (s.e.m.)	Bq/g mean (s.e.m.) × 10000	% of dose mean (s.e.m.)	Bq/g mean (s.e.m.) × 10000	% of dose mean (s.e.m.)
Heart	10.5 (4.7)	0.28 (0.10)	41.9 (5.2)	0.80 (0.03)	47.3 (6.6)	1.04 (0.16)	8.3 (0.7)	0.152 (0.013)
Liver	319 (32)	81.5 (3.4)	211 (25)	53.3 (0.9)	58.7 (3.4)	13.4 (1.5)	476 (22)	82.2 (1.2)
Stomach	2.2 (0.1)	0.19 (0.04)	4.2 (1.5)	0.28 (0.06)	19.1 (0.9)	0.86 (0.11)	5.7 (2.3)	0.274 (0.046)
Intestine	1.7 (0.6)	0.9 (0.1)	6.86 (0.37)	2.99 (0.034)	11.3 (1.1)	4.6 (0.6)	3.8 (0.4)	0.398 (0.023)
Spleen	34 (7)	0.52 (0.03)	38.3 (3.5)	0.43 (0.05)	34.7 (4.0)	0.37 (0.04)	519 (273)	4.2 (1.2)
Lungs	19.9 (9.4)	0.68 (0.20)	102 (10.7)	2.9 (0.4)	95.4 (12.3)	2.4 (0.3)	117 (34)	1.97 (0.13)
Kidneys	34.9 (7.3)	3.6 (0.3)	84.7 (9.18)	6.9 (0.3)	92.8 (18.0)	8.1 (0.7)	43.6 (2.8)	1.25 (0.12)
Blood (/g)	31.6 (15)	12.9 <sup>a</sup> (3.6)	158 (15.7)	51.3 <sup>a</sup> (4.2)	275 (29)	96.6 <sup>a</sup> (8.2)	13.4 (0.5)	3.34 <sup>a</sup> (0.15)
Muscle (/g)	0.52 (0.22)	1.21 <sup>a</sup> (0.29)	2.08 (0.13)	3.9 <sup>a</sup> (0.3)	4.24 (0.09)	8.5 <sup>a</sup> (0.3)	0.98 (0.07)	1.40 <sup>a</sup> (0.03)

<sup>a</sup>The calculation is for total blood or muscle in the mice.

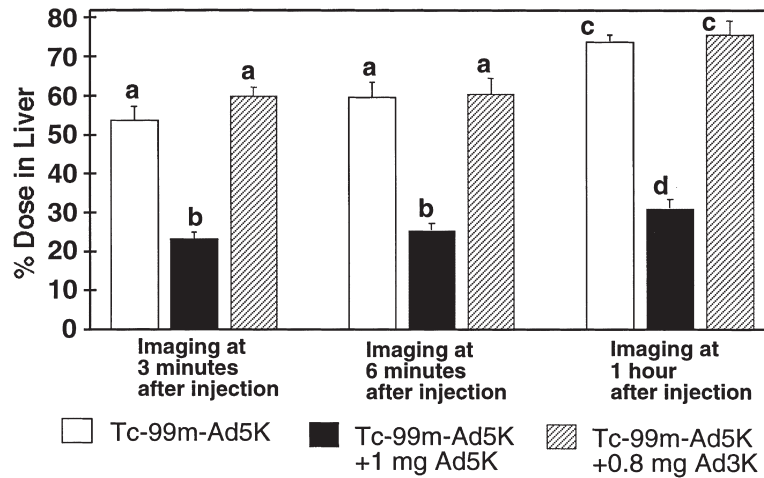


**Figure 5** Liver uptake of <sup>99m</sup>Tc-Ad5K as determined by imaging. Addition of unlabeled Ad5K significantly ( $P < 0.05$ ) reduced the liver accumulation of the <sup>99m</sup>Tc-Ad5K, whereas the addition of unlabeled Ad3K had no effect. Data shown are means ( $n = 4$  per group); the bars are the standard error. Bars with different letters (a, b, c and d) are statistically different at  $P < 0.05$ .

**Table 2** Biodistribution of <sup>99m</sup>Tc-Ad5K 1 h after dosing

Organ or tissue	Mice dosed with <sup>99m</sup> Tc-Ad5K (12 μg)		Mice dosed with <sup>99m</sup> Tc-Ad5K (12 μg) + Ad5K (1 mg)		Mice dosed with <sup>99m</sup> Tc-Ad5K (12 μg) + Ad3K (0.8 mg)	
	Bq/g mean (s.e.m.) × 10 000	% of dose mean (s.e.m.)	Bq/g mean (s.e.m.) × 10 000	% of dose mean (s.e.m.)	Bq/g mean (s.e.m.) × 10 000	% of dose mean (s.e.m.)
Heart	31.1 (5.9)	0.56 (0.04)	47.1 (4.1)	0.98 (0.07)	18.4 (5.9)	0.52 (0.14)
Liver	290 (36)	64.5 (1.5)	99.4 (4.9)	24.3 (2.1)	189 (22)	63.0 (3.3)
Stomach	3.16 (0.42)	0.345 (0.032)	7.4 (1.2)	0.89 (0.19)	3.4 (0.66)	0.410 (0.039)
Intestine	11.5 (3.3)	4.52 (0.56)	14.3 (1.0)	7.37 (0.60)	7.0 (2.1)	4.39 (1.14)
Spleen	27.9 (5.3)	0.297 (0.038)	34.0 (3.1)	0.54 (0.09)	20.6 (4.1)	0.31 (0.03)
Lungs	49.3 (11.0)	1.52 (0.19)	90.5 (8.3)	2.9 (0.2)	30.7 (8.0)	1.35 (0.20)
Kidneys	104 (7.4)	8.16 (0.72)	76.1 (6.3)	6.45 (0.29)	69.6 (8.8)	8.87 (0.96)
Blood (/g)	50.3 (13.8)	15.0 <sup>a</sup> (2.0)	159 (22)	54.3 <sup>a</sup> (5.7)	37.0 (9.6)	17.3 <sup>a</sup> (3.3)
Muscle (/g)	1.76 (0.36)	2.89 <sup>a</sup> (0.21)	4.59 (0.37)	9.1 <sup>a</sup> (1.0)	0.93 (0.20)	2.52 <sup>a</sup> (0.33)

<sup>a</sup>The calculation is for total blood or muscle in the mice.

the 1.3 value at 10 min after dosing. Addition of 1 mg of unlabeled Ad5K reduced the L:B ratio by 10-fold, to  $0.61 \pm 0.08\%$  at 1 h after dosing. The mean value for <sup>99m</sup>Tc-Ad5K with 0.8 mg of unlabeled Ad3K was  $5.1 \pm 1.2$ , not significantly different from that found for <sup>99m</sup>Tc-Ad5K alone. The L:B ratio for <sup>99m</sup>Tc-HSA (mean = 0.21) was significantly lower than all groups dosed with <sup>99m</sup>Tc-Ad5K, indicative of Ad5K binding in the liver. For the 0.6 μg dose of <sup>99m</sup>Tc-Ad5K alone, the L:B ratio averaged 10.0, significantly larger ( $P < 0.05$ ) than the ratio of 1.3 for the 12 μg dose of <sup>99m</sup>Tc-Ad5K.

From Table 2, the percentage of <sup>99m</sup>Tc-Ad5K in total blood averaged 15% for mice killed at 1 h. This value is significantly lower than the 51% blood level for mice killed at 10 min. Therefore, an additional 36% of the dose (4.3 μg) was bound in the liver between 10 and 60 min after dosing.

Additional tissue data presented in Table 2 for <sup>99m</sup>Tc-Ad5K (column 1) are of interest. The uptake of <sup>99m</sup>Tc-Ad5K in the heart ( $3.11 \times 10^5$  Bq/g) was 17.6-fold greater than the uptake in skeletal muscle ( $1.76 \times 10^4$  Bq/g). On a weight basis, the kidney and lung followed liver

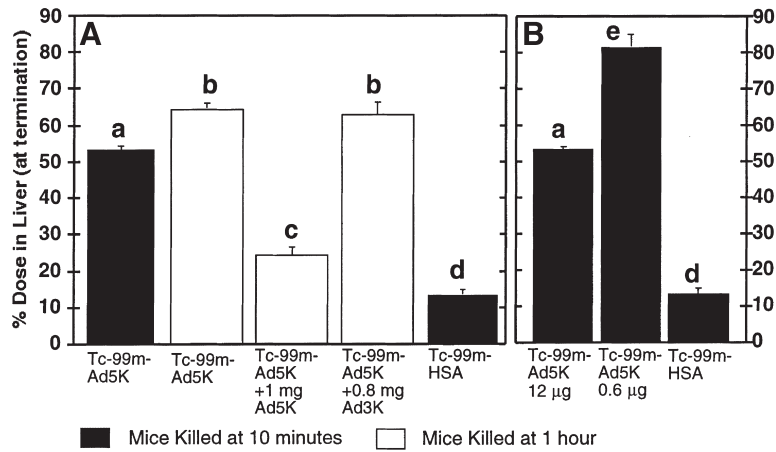


**Figure 6** Liver uptake of <sup>99m</sup>Tc-Ad5K and <sup>99m</sup>Tc-HSA (human serum albumin). Livers were removed at termination (no perfusion) and measured in a gamma counter. Data shown are means (n = 3–4 per group); the bars are the standard error. Bars with different letters (a, b, c, d and e) are statistically different at P < 0.05. (A) Constant 12 µg dose of <sup>99m</sup>Tc-Ad5K. <sup>99m</sup>Tc-Ad5K in liver increased between 10 min and 1 h after injection. Addition of unlabeled Ad5K reduced the liver accumulation of the <sup>99m</sup>Tc-Ad5K, whereas the addition of unlabeled Ad3K had no effect. <sup>99m</sup>Tc-HSA, which indicates the percentage in liver due to blood in the organ, is included in the figure for comparison. (B) Different doses of <sup>99m</sup>Tc-Ad5K. A 0.6 µg dose of <sup>99m</sup>Tc-Ad5K resulted in a higher percentage of liver accumulation at 10 min as compared with a 12 µg dose.

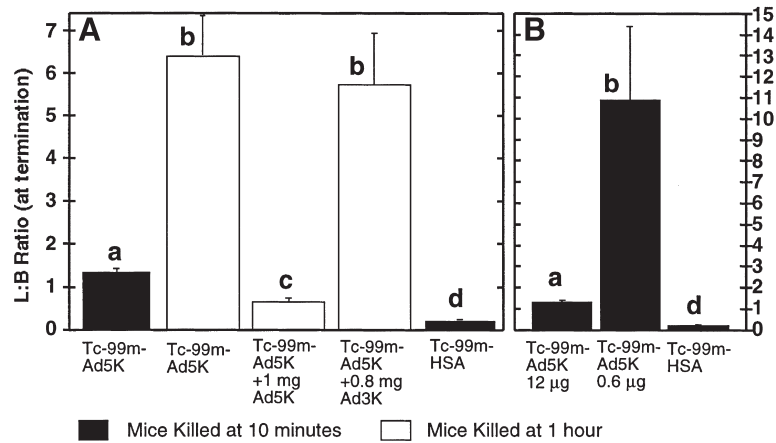


**Figure 7** Liver to blood (L:B) ratios for <sup>99m</sup>Tc-Ad5K and <sup>99m</sup>Tc-HSA (human serum albumin). Livers and blood were removed at termination and measured in a gamma counter. The Bq/g of liver was divided by the Bq/g of blood to obtain the L:B ratio. Data shown are means (n = 3–4 per group); the bars are the standard error. Bars with different letters (a, b, c and d) are statistically different at P < 0.05. (A) Constant 12 µg dose of <sup>99m</sup>Tc-Ad5K. For <sup>99m</sup>Tc-Ad5K alone, the ratio increased between 10 min and 1 h. The ratio was reduced by the addition of unlabeled Ad5K to the <sup>99m</sup>Tc-Ad5K, but was not changed by unlabeled Ad3K. <sup>99m</sup>Tc-HSA, indicating the blood ratio due to blood in the organ, is included in the figure for comparison. (B) Different doses of <sup>99m</sup>Tc-Ad5K. A 0.6 µg dose of <sup>99m</sup>Tc-Ad5K resulted in a higher blood ratio at 10 min as compared with a 12 µg dose.

( $2.9 \times 10^6$  Bq/g) for highest amounts of <sup>99m</sup>Tc-Ad5K binding, averaging  $1.04 \times 10^6$  and  $4.9 \times 10^5$  Bq/g, respectively.

**Liver binding of <sup>99m</sup>Tc-Ad5K modified with anti-Ad5K antibody excess**

Mice were injected with either 1.4 µg of <sup>99m</sup>Tc-Ad5K alone, or with the same dose following preincubation with neutralizing anti-Ad5K antibody (1D6.14, IgG2a) for 45 min (9.4:1 molar ratio of antibody:Ad5K). The excess antibody was sufficient to saturate all binding sites on the Ad5K, since binding analysis indicated that three monoclonal antibody molecules were bound per trimeric knob (data not shown). The mice were imaged repeatedly before termination after 18.5 h; data are summarized in

Figure 8. By 3 min after injection,  $73 \pm 6\%$  of the <sup>99m</sup>Tc-Ad5K dose was detected in the liver region. Preincubation of the <sup>99m</sup>Tc-Ad5K with excess anti-knob antibody significantly ( $P < 0.05$ ) reduced the percentage of liver uptake. At 3 min, the percentage of activity in the liver region for the <sup>99m</sup>Tc-Ad5K + antibody group averaged  $36 \pm 8\%$  of the total animal activity; this same imaging distribution persisted for up to 12 min after injection. By 3.5 h after injection, the anti-Ad5K antibody was less effective in preventing the liver uptake of the <sup>99m</sup>Tc-Ad5K. At 3.5 h, the percentage of activity in the liver region of interest averaged  $92 \pm 7\%$  and  $77 \pm 8\%$ , respectively, for the <sup>99m</sup>Tc-Ad5K alone and <sup>99m</sup>Tc-Ad5K + antibody.

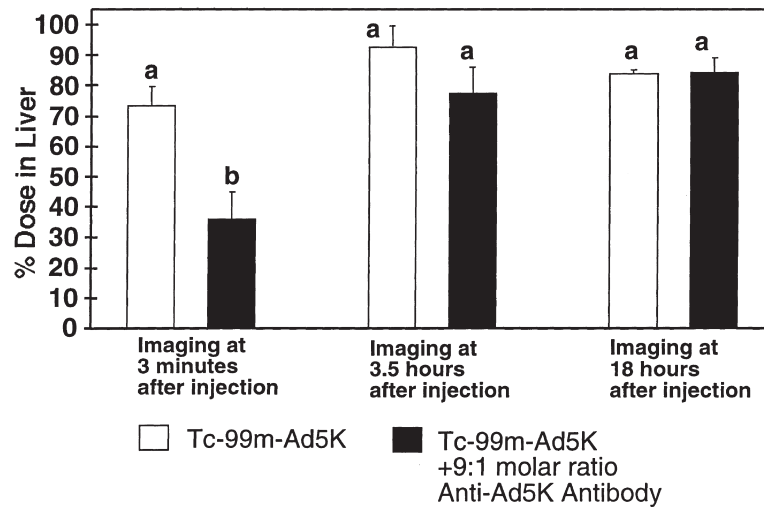


**Figure 8** Liver tropism of <sup>99m</sup>Tc-Ad5K changed with neutralizing antibody. Addition of anti-Ad5K antibody reduced the liver accumulation of the <sup>99m</sup>Tc-Ad5K. Data shown are means ( $n = 4$  per group); the bars are the standard error. Bars with different letters (a and b) are statistically different at  $P < 0.05$ .

Results from biodistribution studies of these two groups of mice are presented in Table 3. Table 3 shows that an average of  $65 \pm 11\%$  of the <sup>99m</sup>Tc-Ad5K alone was retained in the mice at 18.5 h after injection. This implies that the <sup>99m</sup>Tc-Ad5K was metabolized and the <sup>99m</sup>Tc excreted. This is supported as well by the presence of <sup>99m</sup>Tc activity in the intestine. It would appear from the final biodistribution data that anti-Ad5K antibody partially protected the knob from degradation after it localized in the liver. The percentage of activity (per cent dose) for the <sup>99m</sup>Tc-Ad5K (or its degradation products) in

the liver averaged  $35.4 \pm 5.5\%$ , while the <sup>99m</sup>Tc-Ad5K + antibody (or its degradation products) was significantly higher at  $57 \pm 2\%$ .

*Anti-Ad5K antibody targets liver only when pre-incubated with excess Ad5K*

<sup>99m</sup>Tc-anti-Ad5K antibody ( $0.6 \text{ MBq}/\mu\text{g}$  protein) was injected alone ( $10.5 \mu\text{g}$ ) or following preincubation with a 2.1 molar excess of Ad5K. Since each trimeric Ad5K was capable of binding three antibody molecules, the two-fold molar excess of Ad5K insured free binding sites

**Table 3** Biodistribution of <sup>99m</sup>Tc-Ad5K 18.5 h after dosing

Organ or tissue	Mice dosed with <sup>99m</sup> Tc-Ad5K ( $1.4 \mu\text{g}$ )		Mice dosed with <sup>99m</sup> Tc-Ad5K ( $1.4 \mu\text{g}$ ) + anti-Ad5K antibody (9.4:1 molar ratio)	
	Bq/g mean (s.e.m.) $\times 10\,000$	% of dose mean (s.e.m.)	Bq/g mean (s.e.m.) $\times 10\,000$	% of dose mean (s.e.m.)
Heart	0.54 (0.09)	0.049 (0.006)	1.39 (0.892)	0.066 (0.031)
Liver	50.8 (11.6)	35.4 (5.5)	91.3 (15.9)	56.9 (2.1)
Stomach	3.1 (1.3)	2.23 (0.94)	8.54 (3.03)	2.9 (0.8)
Intestine	5.1 (1.5)	6.0 (1.6)	2.67 (0.707)	2.6 (0.5)
Spleen	1.55 (0.25)	0.074 (0.019)	14.3 (5.41)	0.70 (0.11)
Lungs	0.73 (0.15)	0.063 (0.016)	2.31 (1.21)	0.14 (0.04)
Kidneys	6.9 (1.1)	2.1 (0.3)	8.70 (3.71)	1.6 (0.4)
Total		64.6 (11.3)		76.5 (3.7)
Muscle (/g)	0.47 (0.10)	3.08 <sup>a</sup> (0.69)	1.0 (0.5)	4.2 <sup>a</sup> (1.4)

<sup>a</sup>The calculation is for total muscle in the mice.

on the Ad5K for interaction with liver receptors. Therefore, this experiment tested whether the liver uptake of Ad5K was dependent on all three parts of the trimer interacting with the cellular receptor.

The  $^{99m}\text{Tc}$ -antibody alone did not localize to a great extent in the liver. Imaging revealed a relatively unchanged percentage of activity in the liver region over time, averaging  $14.0 \pm 1\%$  immediately before termination at 20 h after dosing. Preincubation with the Ad5K caused the  $^{99m}\text{Tc}$ -antibody to localize in the liver. By 3 min after injection, imaging revealed that  $82 \pm 5\%$  of the dose was liver bound. This percentage increased to  $89 \pm 1\%$  at 20 min after injection and remained at that level until 8 h after injection. Imaging immediately before termination at 20 h after dosing yielded an average of  $86 \pm 3\%$  of the retained activity in the liver. For comparison, analyses of tissues by counting in the gamma counter revealed that the liver uptake of  $^{99m}\text{Tc}$ -labeled antibody (with Ad5K preincubation) averaged  $68.6 \pm 2.6\%$  of the injected dose. This was equal to  $85 \pm 2\%$  of the mean activity retained in the animal at termination and is not significantly different from the  $86 \pm 3\%$  from imaging region of interest analysis. In contrast, the liver uptake of the  $^{99m}\text{Tc}$ -labeled antibody alone averaged  $10.11 \pm 1.51\%$  of the dose.

At 20 h following dosing,  $37.42 \pm 1.78\%$  of the  $^{99m}\text{Tc}$ -anti-Ad5K antibody remained in the blood. By comparison, pre-incubation of the  $^{99m}\text{Tc}$ -labeled antibody with excess Ad5K before injection significantly reduced the blood activity at 20 h down to  $2.26 \pm 0.6\%$  of the injected dose. The Ad5K changed the biodistribution of the  $^{99m}\text{Tc}$ -labeled antibody by causing it to localize in the liver. Further evidence of Ad5K shifting the  $^{99m}\text{Tc}$ -labeled localization to the liver is demonstrated by the L:B ratios. For the  $^{99m}\text{Tc}$ -labeled antibody alone, the ratio averaged  $0.35 \pm 0.03$ . The L:B ratio was significantly increased to  $40.8 \pm 7$  by preincubation of the anti-Ad5K antibody with Ad5K; this represents more than a 100-fold difference.

#### *Liver binding of $^{99m}\text{Tc}$ -Ad5K unchanged when Kupffer cells are inhibited*

Mice ( $n = 3$ ) were injected with  $\text{GdCl}_3$  (10 mg/kg i.v. in saline) at 48 and 24 h before i.v. dosing with  $^{99m}\text{Tc}$ -Ad5K (12  $\mu\text{g}$ ). This dose was previously demonstrated to inhibit liver Kupffer cells in rats and mice.<sup>20–22</sup> The purpose of this experiment was to determine if inhibition of the liver Kupffer cells would change the binding of the  $^{99m}\text{Tc}$ -Ad5K in the liver. Mice were killed after 1 h, biodistribution determined, and results were compared with  $^{99m}\text{Tc}$ -Ad5K without  $\text{GdCl}_3$  pretreatment (Table 2).  $\text{GdCl}_3$  pretreatment had no significant effect on the biodistribution of  $^{99m}\text{Tc}$ -Ad5K. The percentage of  $^{99m}\text{Tc}$ -Ad5K dose present in  $\text{GdCl}_3$ -treated mice tissues averaged  $60.8 \pm 1.5\%$  for the liver,  $0.31 \pm 0.05\%$  for the spleen and  $16.3 \pm 2.4\%$  for total blood.

## *Discussion*

Adenovirus knob (Ad5K) was successfully radiolabeled with  $^{99m}\text{Tc}$  without changing the trimeric structure or specific binding of the molecule to its cellular receptor. Following i.v. injection in mice, the  $^{99m}\text{Tc}$ -Ad5K rapidly localized to the liver in a dose-dependent manner, with specific binding also found in the heart, kidney and lungs. The binding of  $^{99m}\text{Tc}$ -Ad5K in these four tissues

is consistent with the report of Tomko *et al.*<sup>14</sup> that found expression of the Ad5K receptor in these same tissues. Furthermore, the lack of binding of  $^{99m}\text{Tc}$ -Ad5K in skeletal muscle is also consistent with the lack of the Ad5K receptor in this tissue.<sup>14</sup>

Excess anti-Ad5K antibody slowed the liver uptake of  $^{99m}\text{Tc}$ -Ad5K. The liver localization was more completely blocked with excess Ad5K, but not with Ad3K. The rapid localization of  $^{99m}\text{Tc}$ -Ad5K to liver following intravenous dosing is consistent with other reports of the intact adenovirus rapidly localizing to liver when administered by this route.<sup>3,4,23</sup> This is a problem for targeted gene therapy with an adenovirus vector, since the liver removes the adenovirus from the systemic circulation before it reaches the target tissue. Furthermore, expression of the transduced gene in liver may have undesirable consequences.

Dynamic imaging allowed the measurement of time for the  $^{99m}\text{Tc}$ -Ad5K to saturate the liver receptor. The time constant for maximum initial binding (receptor saturation) was calculated to be  $22.7 \pm 3.3$  s. To be meaningful, this value must be compared with the time required for enough blood to flow through the liver to saturate the receptor. Cardiac output and liver blood flow have been reported in unanesthetized mice.<sup>24</sup> Using these values, the cardiac output for the imaged mice would average 20.54 ml per minute, with a liver blood flow of 3.3 ml per minute. Assuming the blood volume was 7% of body weight, the total blood volume would equal 3.05 ml. Therefore, it would take 55.5 s (3.05 ml divided by 3.3 ml per minute) for the entire blood volume to flow through the liver. Dynamic imaging measured the maximum binding to be 29% of the  $^{99m}\text{Tc}$ -Ad5K dose. Assuming complete mixing of the  $^{99m}\text{Tc}$ -Ad5K with blood during the 5–10 s injection time, then the time required for enough blood to flow through the liver to saturate the receptor would be 16.1 s ( $55.5 \text{ s} \times 0.29$ ). Our measured value was 22.7 s in anesthetized mice. The difference between 16.1 s (theoretical maximum) and 22.7 s (dynamic measured value) is probably related to decreased cardiac output by the halothane anesthesia.<sup>25</sup> Therefore, these results would indicate that the  $^{99m}\text{Tc}$ -Ad5K had a 100% extraction efficiency by the liver until receptor saturation and that initial binding was limited only by blood flow to the liver.

Based on experiments with the  $^{99m}\text{Tc}$ -labeled neutralizing anti-Ad5K antibody, binding of Ad5K in the liver does not require that all three subunits of the trimer interact with its cellular receptor. This statement is supported by the following results.  $^{99m}\text{Tc}$ -labeled anti-Ad5K antibody alone did not bind in the liver, since the percentage of dose in the liver was not different than the blood pool agent,  $^{99m}\text{Tc}$ -HSA. When the  $^{99m}\text{Tc}$ -labeled antibody was preincubated with excess Ad5K (2.1 moles Ad5K: 1 mole antibody) and injected into mice, it was rapidly bound in liver. Therefore, the Ad5K caused the  $^{99m}\text{Tc}$ -labeled antibody to bind in the liver, and this occurred in spite of the binding between the antibody and at least one domain of the Ad5K trimer. This implies that all three subunits of the domain are not required for liver binding.

The binding of  $^{99m}\text{Tc}$ -Ad5K in the liver did not appear to be related to a nonspecific uptake mechanism by the RES. This statement is supported by several pieces of evidence. First, binding of  $^{99m}\text{Tc}$ -Ad5K in the spleen was low. Only 0.43 and 0.3% of the  $^{99m}\text{Tc}$ -Ad5K dose was found in the spleen after 10 min and 1 h, respectively.

This is compared with an uptake of 4.2% of the  $^{99m}\text{Tc}$  sulfur colloid dose in the spleen at 10 min. Second, inhibition of the liver Kupffer cells with  $\text{GdCl}_3$  did not change the binding of  $^{99m}\text{Tc}$ -Ad5K in the liver. Furthermore, the  $\text{GdCl}_3$  did not enhance RES activity in the spleen, which has been reported as an effect of the inhibition of Kupffer cells with  $\text{GdCl}_3$ .<sup>26</sup> Third, a dose-dependent binding of  $^{99m}\text{Tc}$ -Ad5K in the liver was found. At 10 min the liver accumulated 81% of a 0.6  $\mu\text{g}$  dose (L:B ratio = 10.0) and only 53% of a 12  $\mu\text{g}$  dose (L:B ratio = 1.3). These results are consistent with binding to a finite number of specific receptors, which is further supported by the fact that adding 1.0 mg of unlabeled Ad5K significantly decreased  $^{99m}\text{Tc}$ -Ad5K binding in the liver while the addition of 0.8 mg unlabeled Ad3K had no effect. If liver binding of  $^{99m}\text{Tc}$ -Ad5K were RES-mediated and decreased uptake were related to overloading the RES system, then it would also be logical to assume that 0.8 mg of Ad3K would also overload the RES system, and decrease binding of  $^{99m}\text{Tc}$ -Ad5K. This was not observed. Finally, pre-incubation of  $^{99m}\text{Tc}$ -Ad5K with excess neutralizing anti-Ad5K antibody blocked liver binding initially. This result can easily be explained by the antibody preventing the  $^{99m}\text{Tc}$ -Ad5K from interacting with its cellular receptor. It would be more difficult to explain how the Ad5K-antibody complex would have less uptake by the RES system, if the Ad5K alone were rapidly bound by the liver RES.

The initial binding capacity of mouse liver for Ad5K averaged 3.1  $\mu\text{g}$ ; after 50 min, the liver binding increased by an additional 4.3  $\mu\text{g}$ . The liver binding capacity for Ad5K (3.1  $\mu\text{g}$ ) is equal to  $3.1 \times 10^{13}$  knob molecules. Mouse liver weights in the dynamic imaging experiments averaged 1.8 g, or  $1.8 \times 10^9$  cells, assuming  $1 \times 10^9$  cells/g tissue. When the average total Ad5K molecules initially bound to liver is divided by the total liver cells, the result is equal to 17000 Ad5K molecules per cell. Assuming saturation of the receptor by  $^{99m}\text{Tc}$ -Ad5K, this value would equal the number of receptors per cell. This value is comparable to the 16000 receptor sites per HeLa cell reported by Wickham *et al*.<sup>17</sup> By contrast Henry *et al*<sup>12</sup> reported 4700 sites per HeLa cell. However, the difference between these values could rest on the fact that measurements reported here are based on *in vivo* determinations.

With 12 Ad5K per adenovirus, the 3.1  $\mu\text{g}$  Ad5K binding capacity by liver would represent  $2.58 \times 10^{12}$  virus particles, assuming each Ad5K binds one receptor. The Ad5K itself had a relatively high affinity for its cellular receptor, as demonstrated here. Since each adenovirus has 12 knobs, the binding affinity of the entire adenovirus should be significantly higher. The higher affinity resulting from multiple knobs on the adenovirus, together with the high liver binding capacity, no doubt contribute to the liver localization. In light of the liver capacity for binding, together with the high affinity for binding, it is likely that gene therapy vectors will need to disrupt the knob domain in order to prevent binding with the cellular receptor in the liver. This would allow the adenovirus to target other tissues by modifications that specifically target other cellular receptors.

## Materials and methods

### Preparation of Ad5 and Ad3 knobs

The knob domains of Ad5 and Ad3 fibers were expressed in *E. coli* with N-terminal 6  $\times$  His tags using the pQE30 expression vector (Qiagen, Hilden, Germany) as described previously.<sup>7</sup> Ad5-Luc 3 DNA and plasmid pBR.Ad3Fib were used as templates for PCR to amplify the DNA encoding the knob domain plus the last repeat of the shaft domain of the respective fiber genes. Primers for these reactions were: F5.F, 5'-TTT AAG GAT TCC GGT GCC ATT ACA GTA GGA A-3'; F5.R, 5'-TAT ATA AGC TTA TTC TTG GGC AAT GTA TGA-3'; F3.F, 5'-CTC GGA TCC AAT TCT ATT GCA CTG AAA AAT AAC-3'; and F3.R, 5'-GGG AAG CTT AGT CAT CTT CTC TAA TAT AGG AAA AGG-3'. The PCR products were digested with *Bam*HI and *Hind*III and cloned into *Bam*HI-*Hind*III-digested pQE30, resulting in plasmids pQE.KNOB5 and pQE.KNOB3. Recombinant knobs were expressed in *E. coli* M15(pREP4) cells harboring pQE.KNOB5 or pQE.KNOB3 and purified on Ni-NTA agarose columns (Qiagen). The concentrations of the purified knobs were determined by the Bradford protein assay (BioRad, Hercules, CA, USA). The ability of each recombinant knob to form a homotrimer was verified by SDS-PAGE of unboiled samples. The ability of each recombinant knob to block infection by the adenovirus of corresponding serotype was verified as described previously.<sup>7</sup>

### Radiolabeling and SDS-PAGE

Recombinant Ad5K, with an N-terminal 6 histidine tag, was modified with succinimidyl 6-hydrazinonicotinate (HYNIC, 5:1 molar ratio, 3–4 h) and dialyzed overnight against PBS.<sup>27</sup> Anti-Ad5K monoclonal antibody (1D6.14, IgG2a) was also modified with HYNIC.<sup>5</sup> The modified proteins were radiolabeled with  $^{99m}\text{Tc}$  using tricine as the transfer ligand and purified from nonbound  $^{99m}\text{Tc}$  by G-25 size exclusion chromatography.<sup>28</sup> Protein concentrations of the collected fractions were determined by the method of Lowry.<sup>29</sup> The protein-bound  $^{99m}\text{Tc}$  was evaluated by thin-layer chromatography (TLC). The chromatography strips (1  $\times$  8 cm) were spotted with protein at one end, eluted with either saline or methyl ethyl ketone as the mobile phase, then cut into 2 mm pieces before counting in a gamma counter. Protein-bound  $^{99m}\text{Tc}$  did not move with either solvent. The  $^{99m}\text{Tc}$ -labeled Ad5K was subjected to SDS-PAGE, using a 12–20% gradient, under nonreducing conditions without heat.

### In vitro assays

Binding assays were conducted using U293 cells, with and without a 100-fold excess of Ad5K. Scatchard plots of specific binding of the  $^{99m}\text{Tc}$ -Ad5K to the U293 cells was analyzed using the Ligand program.<sup>30</sup> Following decay of the  $^{99m}\text{Tc}$ , the Ad5K was assayed for biological activity to inhibit infection of U293 cells with Ad5.

### Animal injections and tissue preparation

The  $^{99m}\text{Tc}$ -Ad5K (or anti-Ad5K antibody) was intravenously injected into 12-week-old male CD1 mice (tail vein) under halothane anesthesia. There were at least three mice per treatment group. Syringes were counted before and after injection using a Atomlab 100 dose cali-

brator (Biodex Medical Systems, Shirley, NY, USA). At termination, the tissues were collected, weighed and counted in a Minaxiγ Auto-Gamma 5000 series gamma counter (Packard, Downers Grove, IL, USA). After the tissues were removed, the remaining carcass was subdivided into three vials for counting. The tail was also counted separately to prove intravenous dosing. Samples that counted greater than 37 000 Bq were recounted after appropriate decay, since the gamma counter's response was not linear beyond that count rate.

#### *Imaging and region of interest analysis*

The mice were imaged with an Anger 420/550 Mobile Radioisotope Gamma camera (Technicare, Solon, OH, USA), equipped with a pinhole collimator. Mice were imaged repeatedly for up to 20 h after injection, using both dynamic and single image planar imaging techniques. During imaging, the mice were maintained with halothane anesthesia and positioned in dorsal recumbency with the legs extended from the body. For dynamic studies, the mouse was positioned for imaging and had image acquisition started (5 s per frame for 60 total frames) upon intravenous injection of the  $^{99m}\text{Tc}$ -Ad5K. For single image sessions the mice were imaged for a length of 2–30 min. The length of image time was varied depending on the dose and decay of the  $^{99m}\text{Tc}$ . The image time was adjusted to allow for collection of at least 50 000 total counts.

Images were processed on a Pegasys processing system (ADAC Laboratories, Milpitas, CA, USA) using standard region of interest analysis. Three regions of interest were drawn: heart, liver and whole animal. A background region was drawn outside the animal image to correct the whole body and liver regions for background counts. Total counts and pixels were recorded for all regions. The average count per pixel for the background region was multiplied by the pixels in the whole animal and liver regions of interest; that number was then subtracted from the counts in each respective region.

The liver region was also corrected for blood pool. This was accomplished by injecting mice ( $n = 3$ ) with  $^{99m}\text{Tc}$ -labeled HSA, a commonly used blood pool agent in nuclear medicine, and conducting identical dynamic and static imaging protocols as described. The heart to blood ratio from region of interest analysis was determined to be 1.30. Therefore, counts in the heart region were multiplied by 1.3, then subtracted from the liver in order to correct for blood in the liver. Since the  $^{99m}\text{Tc}$ -Ad5K and anti-Ad5K antibody did not bind appreciably in the heart, any detected activity in that region of interest was assumed to be from blood. As shown in Figure 3, the  $^{99m}\text{Tc}$ -Ad5K in the liver rapidly decreased to zero and became negative, as the dose was present in the heart. The negative values were due to the correction for  $^{99m}\text{Tc}$ -Ad5K in blood, using the heart region of interest. Initially, the dose was present in the heart and had not yet reached equilibrium with the circulation.

Finally, the fraction of activity in the liver region was calculated as the ratio between the background and blood corrected counts in the liver region, divided by the background corrected counts in the whole animal.

#### *Data reduction for tissues collected at termination*

The raw count rate data from the gamma counter were decay corrected to the injection time and converted to

activity using absolute efficiency corrections. Since the entire mouse was counted in the gamma counter, the sum of the decay corrected activities for all tissues and carcass (not including tail) was considered the total dose, provided no radioactivity was excreted (10 min and 1 h time-points). If excretion had occurred, then the dose was determined by the dose calibrator measurements of the syringe, before and after dosing. The rationale for choosing the sum of the gamma counter measurements for calculating total dose was that the precise amount in the tail could be measured, and excluded as part of the dose. This was deemed more accurate, since it corrected for radioactivity not intravenously injected or any external leakage at the injection site. Tail radioactivity was less than 10% of the dose since bad injections were readily identified from the initial gamma camera imaging. Consequently, additional mice could be injected as needed.

Radioactivity in tissues was normalized to the tissue weight, as well as to the percentage of dose as described above. The total radioactivity was estimated for blood and muscle by assuming a total mass equal to 7% and 40% of body weight, respectively.

Since the mice were not perfused when they were killed, part of the tissue radioactivity was due to blood in that tissue. An index of specific uptake is represented with the tissue:blood ratio, which is the activity per gram of tissue divided by the activity per gram of blood.

Statistical comparisons were made using the analysis of variance protocol (Proc GLM) in the SAS analysis package.<sup>31</sup>

### *Acknowledgements*

This work was primarily supported by Sankyo Co. Ltd and in part by the following grants: NIH contract N01-AR-6-2224, NIH grant RO1 H1/KDK 50255, NIH grant R01-CA 74242, and US Army, Department of Defense, DAMD 17-94J 4398.

### *References*

- 1 Stratford-Perricaudet LD, Makeh I, Perricaudet M, Briand P. Widespread long-term gene transfer to mouse skeletal muscles and heart. *J Clin Invest* 1992; **90**: 626–630.
- 2 Herz J, Gerard RD. Adenovirus-mediated transfer of low density lipoprotein receptor gene acutely accelerates cholesterol clearance in normal mice. *Proc Natl Acad Sci USA* 1993; **90**: 2812–2816.
- 3 Kass-Eisler A *et al.* The impact of developmental stage, route of administration and the immune system on adenovirus-mediated gene transfer. *Gene Therapy* 1994; **1**: 395–492.
- 4 Huard J *et al.* The route of administration is a major determinant of the transduction efficiency of rat tissues by adenoviral recombinants. *Gene Therapy* 1995; **2**: 107–115.
- 5 Douglas JT *et al.* Targeted gene delivery by tropism-modified adenoviral vectors. *Nat Biotech* 1996; **14**: 1574–1578.
- 6 Goldman CK *et al.* Targeted gene delivery to Kaposi's sarcoma cells via the fibroblast growth factor receptor. *Cancer Res* 1997; **57**: 1447–1451.
- 7 Krasnykh VN, Mikheeva GV, Douglas JT, Curiel DT. Generation of recombinant adenovirus vectors with modified fibers for altering viral tropism. *J Virol* 1996; **70**: 6839–6846.
- 8 Michael SI, Hong JS, Curiel DT, Engler JA. Addition of a short peptide ligand to the adenovirus fiber protein. *Gene Therapy* 1995; **2**: 660–668.

- 9 Wickham TJ, Roelvink PW, Brough DE, Kovessi I. Adenovirus targeted to heparin-containing receptors increases its gene delivery efficiency to multiple cell types. *Nat Biotech* 1996; **14**: 1570–1573.
- 10 Wickham TJ *et al*. Targeted adenovirus gene transfer to endothelial and smooth muscle cells by using bispecific antibodies. *J Virol* 1996; **70**: 6831–6838.
- 11 Bergelson JM *et al*. Isolation of a common receptor for coxsackie B viruses and adenoviruses 2 and 5. *Science* 1997; **275**: 1320–1323.
- 12 Henry LJ *et al*. Characterization of the knob domain of the adenovirus type 5 fiber protein expressed in *Escherichia coli*. *J Virol* 1994; **68**: 5239–5246.
- 13 Louis N *et al*. Cell-binding domain of adenovirus serotype 2 fiber. *J Virol* 1994; **68**: 4104–4106.
- 14 Tomko RP, Xu R, Philipson L. HCAR and MCAR: the human and mouse cellular receptors for subgroup C adenoviruses and group B coxsackieviruses. *Proc Natl Acad Sci USA* 1997; **94**: 3352–3356.
- 15 Hong SS *et al*. Adenovirus type 5 fiber knob binds to MHC class I  $\alpha 2$  domain at the surface of human epithelial and B lymphoblastoid cells. *EMBO J* 1997; **16**: 2294–2306.
- 16 Bai M, Harfe B, Freimuth P. Mutations that alter an Arg–Gly–Asp (RGD) sequence in the adenovirus type 2 penton base protein abolish its cell-rounding activity and delay virus reproduction in flat cells. *J Virol* 1993; **67**: 5198–5205.
- 17 Wickham TJ, Mathias P, Cheresch DA, Nemerow GR. Integrins  $\alpha v \beta 3$  and  $\alpha v \beta 5$  promote adenovirus internalization but not virus attachment. *Cell* 1993; **73**: 309–319.
- 18 Defer C, Belin MT, Caillet-Boudin ML, Boulanger P. Human adenovirus-host cell interactions: comparative study with members of subgroups B and C. *J Virol* 1990; **64**: 3661–3673.
- 19 Stevenson SC *et al*. Human adenovirus serotypes 3 and 5 bind to two different cellular receptors via the fiber head domain. *J Virol* 1995; **69**: 2850–2857.
- 20 Roerdink F *et al*. The involvement of parenchymal, Kupffer, and endothelial liver cells in the hepatic uptake of intravenously injected liposomes. Effects of lanthanum and gadolinium salts. *Biochim Biophys Acta* 1981; **677**: 79–89.
- 21 Lazar G Jr *et al*. Inhibition of anaphylactic shock by gadolinium chloride-induced Kupffer cell blockade. *Agents Actions* 1994; **41**: C97–98.
- 22 Louis H *et al*. Hepatoprotective role of interleukin 10 in galactosamine/lipopolysaccharide mouse liver injury. *Gastroenterology* 1997; **112**: 935–942.
- 23 Worgall S, Wolff G, Falck-Pedersen E, Crystal RG. Innate immune mechanisms dominate elimination of adenoviral vectors following *in vivo* administration. *Hum Gene Ther* 1997; **8**: 37–44.
- 24 Wang P, Zheng FB, Burkhardt J, Chaudry IH. Trauma-hemorrhage and resuscitation in the mouse: effects on cardiac output and organ blood flow. *J Physiol* 1993; **264**: H1166–H1173.
- 25 Frink EJ *et al*. The effects of sevoflurane, halothane, enflurane, and isoflurane on hepatic blood flow and oxygenation in chronically instrumented greyhound dogs. *Anesthesiology* 1992; **76**: 85–90.
- 26 Vollmar B *et al*. Modulation of Kupffer cell activity by gadolinium chloride in endotoxemic rats. *Shock* 1996; **6**: 434–441.
- 27 Abrams MJ *et al*. Technetium-99m-human polyclonal IgG radiolabeled via the hydrazino nicotinamide derivative for imaging focal sites of infection in rats. *J Nucl Med* 1990; **21**: 2022–2028.
- 28 Larsen SK, Solomon HF, Caldwell G, Abrams MJ. [<sup>99m</sup>Tc]Tricine: a useful precursor complex for the radiolabeling of hydrazino-nicotinate protein conjugates. *Bioconj Chem* 1995; **6**: 635–638.
- 29 Lowry OH, Rosebrough NJ, Farr LA, Randall RJ. Protein measurement with the folin phenol reagent. *J Biol Chem* 1951; **193**: 265–275.
- 30 Munson P, Rodbard D. LIGAND: a versatile computerized approach for characterization of ligand binding systems. *Anal Biochem* 1980; **107**: 220–239.
- 31 Statistical Analysis System (SAS), Release 6.11, SAS Institute Inc., Cary, NC, USA.